PAPER

Highly conductive and transparent Ag honeycomb mesh fabricated using a monolayer of polystyrene spheres

To cite this article: Namyong Kwon *et al* 2013 *Nanotechnology* **24** 235205

Nanotechnology **24** (2013) 235205 (8pp) doi:10.1088/0957-4484/24/23/235205

Highly conductive and transparent Ag honeycomb mesh fabricated using a monolayer of polystyrene spheres

Namyong Kwon[1,4], **Kyohyeok Kim**[1,4], **Sihyun Sung**[2], **Insook Yi**[3] and **Ilsub Chung**[1,2]

[1] SKKU Advanced Institute of Nanotechnology, Sungkyunkwan University, Suwon 440-746, Korea
[2] College of Information and Communication Engineering, Sungkyunkwan University, Suwon 440-746, Korea
[3] Advanced Technology Team, InkTec Technology Center, Ansan 425-839, Korea

E-mail: ichung@skku.ac.kr

Received 5 March 2013, in final form 4 April 2013
Published 15 May 2013
Online at stacks.iop.org/Nano/24/235205

Abstract
We describe the design principles and fabrication of Ag honeycomb mesh as a transparent conductive electrode using a polystyrene (PS) sphere template. Monolayers of PS spheres with different diameters, such as 600 nm, 3 μm, and 10 μm, are studied as templates to form Ag mesh with high transmittance. Since the parasitic Ag islands degrade the transmittance, both heat pretreatment and wet etching are used to control the area covered by parasitic Ag islands. The trade-off between transmittance and conductivity forces us to use larger diameter PS spheres. Ten-micron PS spheres are chosen as the template for the PS sphere monolayer, and heat pretreatment and Ag wet etching are used to demonstrate that the Ag honeycomb mesh transparent electrodes have high performance. The transmittance and the sheet resistance are 83% and 20 Ω/sq, which are comparable to commercial ITO electrodes.

S Online supplementary data available from stacks.iop.org/Nano/24/235205/mmedia

(Some figures may appear in colour only in the online journal)

1. Introduction

Thin transparent conducting films are crucial for liquid crystal displays (LCDs), flat panel displays, touch panels, organic light-emitting diodes (OLEDs), solar cells, smart windows, and other applications [1–3]. Currently, indium tin oxide (ITO), a transparent conducting oxide (TCO), is the industry standard due to its low resistivity (10^{-3}–10^{-4} Ω cm) and high transparency in the visible spectrum (80%–90%). However, ITO has many disadvantages, such as rarity, high cost, possible exhaustion, process temperature limitations, and brittleness on a flexible substrate [1–3]. In particular, as display technology moves toward flexible displays, ITO will become completely unsuitable due to its brittleness.

To address these issues, many researchers have been studying ITO substitutes. In recent efforts, metal nanowires [4, 5], conducting polymers [6, 7], carbon nanotube networks [8, 9], graphene films [10], hybrid thin films [11–15], and metal meshes/grids [16–22] have been evaluated as candidates to replace ITO electrodes. Among these various materials, silver nanowire thin films are the leading alternative to ITO due to good transmittance, conductivity, and flexibility [4, 5]. Conductive polymers have relatively poor transmittance and conductivity, though these have improved significantly in recent years [7]. Carbon nanotube networks have excellent transmittance, but are currently limited to a sheet resistance of about 300 Ω/sq by high contact resistance [9]. Graphene is a promising technology due to its exceptionally good transmittance, conductivity, and flexibility. However, it has the fatal disadvantages that large area sheets cannot be printed and manufacture is currently expensive and time intensive,

[4] These authors contributed equally to this work.

as it requires chemical vapor deposition using a copper film catalyst [10]. Recently, hybrid films have been intensively studied by mixing two materials, such as ITO with Ag film [11], ITO with carbon nanotubes [12], polymer with carbon nanotubes [13], Ag nanowire with polymers [14], and graphene with polymers [15]. However, this research is at an early stage and the production process is complicated. Finally, metal grid/mesh is extremely conductive and can be produced in a roll-to-roll process on a large scale, but has low transmittance and non-uniform coverage at the nanoscale as the metal wire is about 10 μm in diameter [16]. In recent years, metal mesh electrodes with diameters less than 1 μm, which have been fabricated using the nanoimprint method or microtransfer molding, have possessed maximum transparencies below 80% (at 550 nm) [17, 18]. Even though these results are relatively good, commercial production is limited due to sample size and an expensive vacuum process.

Polystyrene (PS) lithography and its applications have been intensively studied in recent years [19–29]. This method could be used to create an ITO substitute with high transmittance and good sheet resistance in the form of a honeycomb mesh, which seems to be effective for transparent electrodes [19–21]. Some efforts to fabricate conductive meshes using PS spheres have been made. Wei *et al* reported transparent conductive metallic electrodes on glass using a PS sphere template [19]. They deposited a thin Al film (20 nm thick) using PS spheres (300 nm in diameter) as masks, thereby fabricating a metallic hole array with an optical transmittance of 65% and sheet resistance of 6 Ω/sq. Cheng *et al* demonstrated Au nanomesh using PS spheres (600 nm in diameter) as etching masks, but the transparency was 72% [20]. Perng *et al* fabricated a nickel oxide honeycomb nanomesh for nanostructure devices [21]. These materials, however, are not suitable for commercial mass production due to the use of a high cost vacuum process or small sample sizes. Furthermore, these works do not fully exploit the unique properties of metal meshes: high transmittance with low sheet resistance. The limited transmittance of metal mesh films could be due to the relatively small holes in the mesh. Therefore, construction of metal mesh with large holes on a large scale is critical for commercial production as an ITO substitute.

In this study, a new architecture for transparent electrodes consisting of a Ag honeycomb mesh is described. A self-assembled monolayer of polystyrene spheres was formed as a template to create the mesh pattern and coated with Ag ink using a manually operated bar. The Ag honeycomb mesh was examined by measuring transmittance and sheet resistance. Since they degrade transmittance, pretreatment and Ag wet etching were used to minimize or eliminate Ag parasitic islands near Ag mesh lines. In addition, larger diameter PS spheres created larger holes and thicker Ag lines.

2. Experimental details

2.1. Formation of a PS sphere monolayer

A 150 μm-thick poly(ethylene terephthalate) (PET) substrate was plasma treated to obtain a hydrophilic surface (contact angle about 50°). 600 nm and 3 μm PS spheres at 10 wt% in water solution were purchased from Sigma Aldrich and 10 μm PS spheres crosslinked with divinylbenzene were purchased from Polyscience, Inc. at 2.66 wt% in water solution. The PS spheres were extracted by eliminating the water using centrifugation. Then, the PS spheres were put in ethanol to form a 20–30 wt% ethanol solution. As shown in figure S1 (available at stacks.iop.org/Nano/24/235205/mmedia), a periodic hexagonal close-packed monolayer of PS spheres was formed using a modified floating transferring method [22, 23]. We filled a water tank (200 mm × 300 mm × 50 mm) with deionized (DI) water. When a PS solution was dropped at the interface of the DI water and air, the PS spheres rapidly spread and self-assembled into a PS sphere monolayer on the DI water surface. After dropping a proper amount of PS solution, the monolayer was condensed by pushing it toward the wall using a bar. As shown in figures S1(c) and (d) (available at stacks.iop.org/Nano/24/235205/mmedia), once the condensed monolayer was formed on the water surface, the bar was pushed at the same speed to keep the monolayer condensed. Finally, the transferred PS sphere monolayer on the PET substrate was dried by removing the DI water with heat. The PS sphere semi-monolayer film was 200 mm × 150 mm.

2.2. Fabrication of the Ag honeycomb mesh

Ag ink (10 ml, 11.5 wt%, TEC-IJ-010, Inktec) was dropped onto the surface of the PS sphere monolayer film on the PET substrate and uniformly coated by pushing a bar. The Ag was cured in a two-step annealing process at 100 °C for 5 min followed by 140 °C for 10 min on a hot plate. The PS sphere monolayer film was lifted off by sonicating for 3 min in toluene.

2.3. Ag wet etching

The Ag was wet etched by immersing the Ag honeycomb mesh in nitric acid (20 wt%) to remove parasitic Ag islands as a function of the accumulated time. After wet etching, the sample was immersed into DI water and blown with nitrogen gas.

2.4. Heat pretreatment

The monolayer of PS spheres on the PET substrate was partially melted on a hot plate before the Ag ink coating process. The specific temperature was a function of the PS sphere diameter. The heat pretreatment temperatures for 3 μm and 10 μm PS spheres were 110 °C and 150 °C, respectively.

2.5. Characterization

SEM images of PS sphere monolayers and Ag honeycomb meshes were obtained using field emission scanning electron microscopy (JSM-7401F, JEOL). The detailed morphological analyses and current images of the Ag honeycomb were collected using a scanning probe microscope (SPA-300, Seiko Instruments) by probing with cantilevers (Si-DF40 and AF1 with Au coating). In addition, an image-processing program

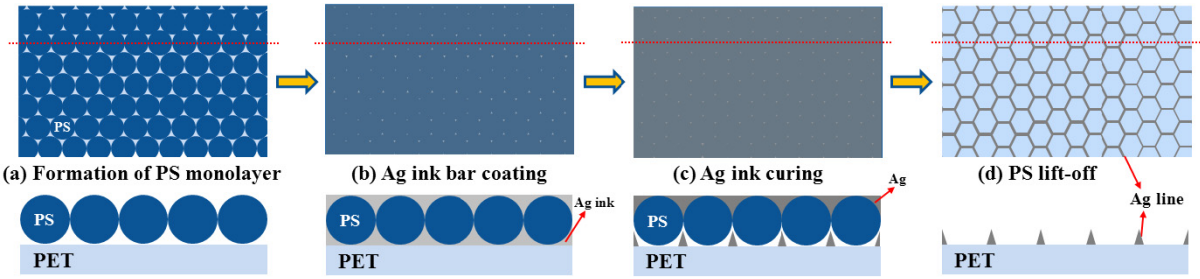

Figure 1. Schematic process flow to fabricate Ag honeycomb mesh using a PS sphere monolayer.

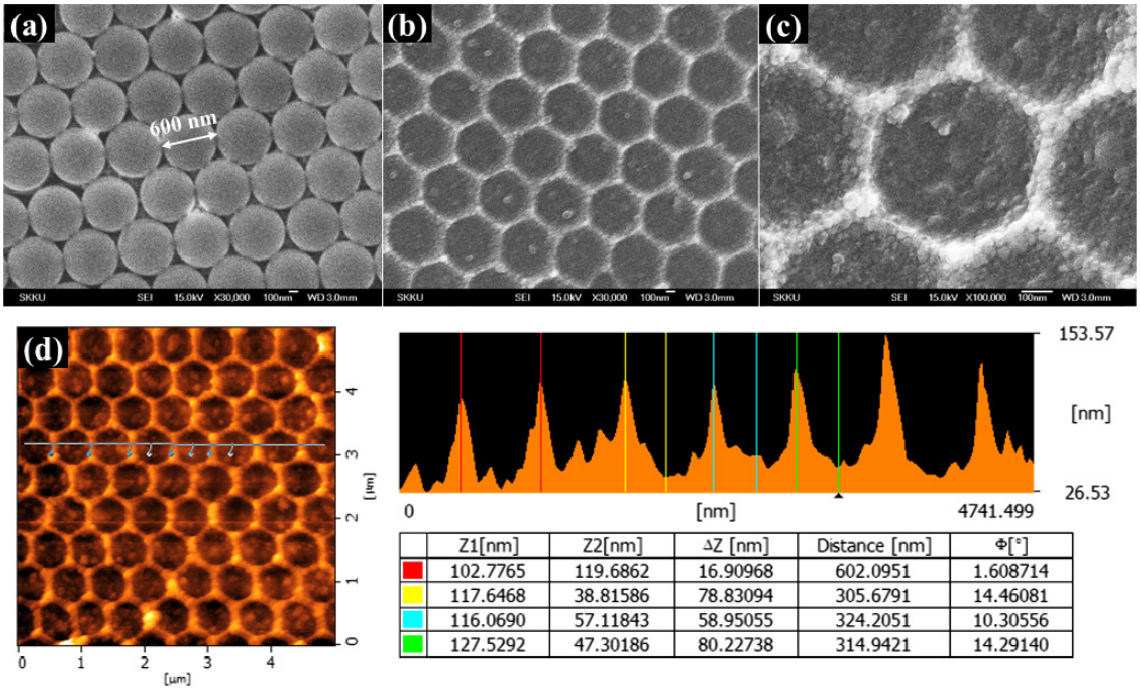

	Z1[nm]	Z2[nm]	ΔZ [nm]	Distance [nm]	Φ[°]
	102.7765	119.6862	16.90968	602.0951	1.608714
	117.6468	38.81586	78.83094	305.6791	14.46081
	116.0690	57.11843	58.95055	324.2051	10.30556
	127.5292	47.30186	80.22738	314.9421	14.29140

Figure 2. FE-SEM images of (a) a monolayer of 600 nm PS spheres and ((b), (c)) the Ag honeycomb mesh obtained after the lift-off process. (d) SPM images and analyzed thickness profile scanned to line.

(TOMORO SCOPE-EYE) was used to accurately analyze the Ag honeycomb mesh dimensions. Sheet resistance and transmittance were obtained using a sheet resistance meter (FPP-2000, DASOL ENG) and transmittance meter (MTR-2, 3M), respectively.

3. Results and discussion

3.1. Ag mesh fabricated with 600 nm PS spheres

Figure 1 illustrates a schematic of the process to fabricate a Ag honeycomb mesh using a PS sphere monolayer. First, a close-packed PS sphere monolayer was formed on a PET substrate using the floating transferring method [22, 23]. Additionally, a hot plate was used to pretreat and melt the PS spheres partially. Then, Ag ink (11.5 wt%, TEC-IJ-010, Inktec) was dropped onto the PS film surface and uniformly coated using a bar. Subsequently, a two-step Ag curing process was performed. Finally, a lift-off process was used to obtain the Ag mesh. Details of the process are described in section 2.

As an initial experiment, we fabricated a Ag honeycomb mesh with 600 nm PS spheres. The PS sphere monolayer was formed on the PET substrate as shown in figure 2(a). The Ag honeycomb mesh was obtained after Ag ink coating and PS sphere lift-off, as shown in figures 2(b) and (c). Scanning probe microscopy (SPM) (figure 2(d)) indicated that the distance between parallel lines of Ag mesh was about 600 nm, which is the diameter of the PS spheres. In addition, the Ag lines ranged from about 60 to 80 nm thick, as shown in figure 2(d). The transmittance was about 20%, and the sheet resistance was above 2000 Ω/sq. The SPM topologies and SPM current images of the Ag honeycomb mesh were obtained (see the supporting information, figure S2 available at stacks.iop.org/Nano/24/235205/mmedia). Using these current images, we confirmed that little current (below 1 nA) flowed through the Ag honeycomb mesh (supporting information, figures S2(c) and (d) available at stacks.iop.org/Nano/24/235205/mmedia). To determine the cause of the poor conductivity of the Ag honeycomb mesh, we measured the current at seven different positions on the Ag mesh with

sweeping voltage from −3 to 3 V. The slope of the *I*–*V* curves, given in figure S2(e) (available at stacks.iop.org/Nano/24/235205/mmedia), represents the resistance between two probe positions that are cantilevered contacts with a common ground. The measured resistances ranged from about 3 to 7 GΩ; these values are too large for conductive electrodes. The SPM analysis indicated that the conductivity was poor because the Ag lines were too thin. Current images were obtained by biasing 1 V with a Au coated cantilever (AF1 tip). Thus, larger PS spheres are needed to retain more Ag ink in the spaces between PS spheres, which will yield thicker Ag mesh. The poor transmittance (about 20%) was also surprising. Two factors could yield such poor transmittance. The most noticeable factor was the parasitic Ag islands between mesh patterns, as shown in figure 2(c). To improve the transmittance, an additional process like wet etching is necessary to eliminate parasitic Ag islands. The second factor degrading the transmittance was light scattering due to the small patterns. When the Ag mesh holes are smaller than 600 nm, incident visible light (400–800 nm) can be scattered because the holes are too small, thereby decreasing transmittance [19, 20]. Thus, we used wet etching to eliminate parasitic Ag islands, and used larger PS spheres to obtain better conductivity.

3.2. Heat pretreated, 3 μm PS spheres combined with wet etching

A PS sphere monolayer and a Ag honeycomb mesh were created using 3 μm PS spheres (figure 3). The measured transmittance was about 35%, and the sheet resistance was less than 30 Ω/sq. In addition to light scattering, the poor transmittance of the Ag honeycomb mesh created using 3 μm PS spheres is attributed to parasitic Ag islands. Parasitic Ag islands can form in all spaces between PS spheres because Ag ink penetrates all the empty spaces between PS spheres [24]. Ag parasitic islands were mostly nucleated near Ag lines when the Ag solution evaporated. Ag parasitic islands could be eliminated using either dry etching or wet etching. The easiest approach to minimize Ag parasitic islands was wet etching.

The Ag parasitic islands were etched by immersing the Ag honeycomb mesh in 20 wt% nitric acid. The transmittance and sheet resistance were measured at different spots and averaged as a function of the accumulated etching time. The transmittance was measured without considering the light absorbance of the PET substrate. As shown in figure 3(d), the transmittance before wet etching was 35%, while the transmittance after wet etching for 900 s was 57%. Wet etching improved the transmittance by about 22 percentage points. During the initial etching period (0–100 s), the transmittance increased rapidly because relatively thin parasitic Ag islands were removed quickly. After the initial etching period, the transmittance increased monotonically because relatively thick parasitic Ag islands were eliminated slowly. The initial sheet resistance before wet etching was 30 Ω/sq. In the early etching period, the sheet resistance decreased from 30 to 8 Ω/sq due to eliminating oxidized residues and by-products. However, the sheet resistance

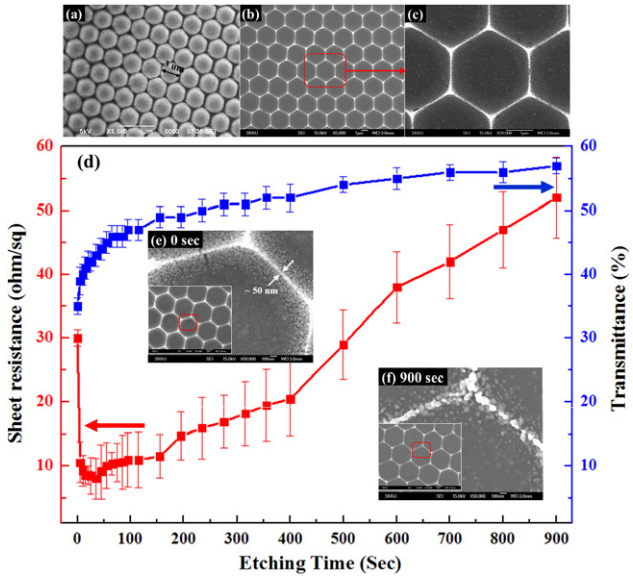

Figure 3. FE-SEM images of (a) a 3 μm PS sphere monolayer and (b) a Ag honeycomb mesh. (c) Enlargement of the dotted box in (b). (d) Variation in sheet resistance and transmittance of Ag honeycomb mesh fabricated using 3 μm PS by etching time. FE-SEM images and enlarged images of Ag honeycomb mesh (e) before etching and (f) after etching for 900 s. Enlarged FE-SEM image areas are indicated by dashed boxes.

increased as the etching time increased due to the decreased Ag line thickness, thereby yielding 52 Ω/sq after etching for 900 s. Figures 3(e) and (f) show field emission scanning electron microscopy (FE-SEM) images of Ag mesh before and after Ag etching. The width of the Ag lines and the parasitic Ag island density tend to decrease as the wet etch time increases. Before wet etching, the parasitic Ag islands were distributed near Ag lines, about 500 nm apart, while the main Ag lines were about 50 nm wide. After wet etching for 900 s, the Ag line thickness decreased from about 197 to about 147 nm; about 50 nm of Ag was eliminated (supporting information, figure S3 available at stacks.iop.org/Nano/24/235205/mmedia). As a result, as shown in figure 3(f), a considerable number of Ag parasitic islands near Ag lines were removed. Unfortunately, the Ag lines were also etched, leaving thin or broken Ag lines. The reduced parasitic Ag islands increased the transmittance from 35% to 57%. The thin and broken Ag lines, however, contributed to an increased sheet resistance from 30 to 52 Ω/sq after etching for 900 s. Consequently, we confirmed that the increased sheet resistance to over 50 Ω/sq was due to the decreased Ag line thickness. Thus, the area of parasitic Ag islands should be minimized and the Ag line thickness should be maximized if wet etching is used effectively.

In an effort to minimize the area of parasitic Ag islands, a new process called heat pretreatment was examined in terms of temperature and time. Heat pretreatment was performed using a hot plate to control the empty volume between the PS spheres and the PET. Schematic cross-sectional diagrams of pretreated and untreated PS spheres were compared (figure 4). As shown in figure 4(a), Ag lines formed in the central areas between the PS spheres and parasitic Ag islands formed

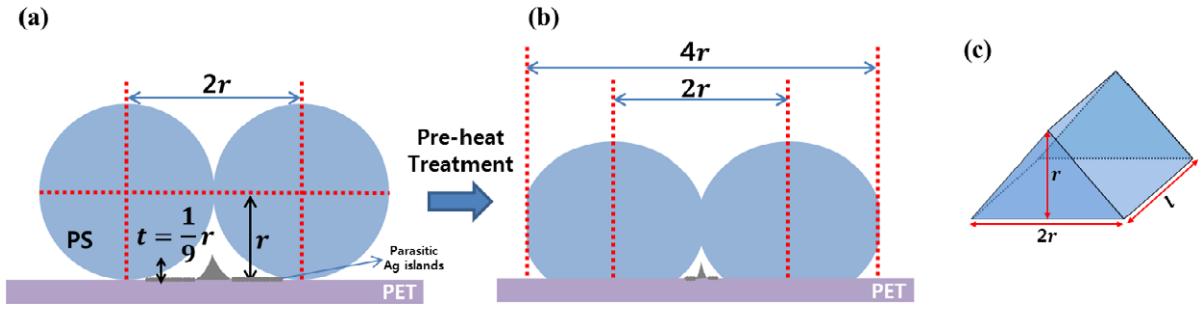

Figure 4. Schematic cross-sectional diagram of Ag mesh (a) without heat pretreatment and (b) with heat pretreatment. (c) The triangular prism of the empty space.

in all areas between the PS spheres as the Ag ink solvent evaporated. However, when the PS spheres were annealed on the PET substrate, the empty space between the PS spheres and the PET surface decreased and fewer parasitic Ag islands formed, as shown in figure 4(b). To predict the effect of heat pretreatment on volume shrinkage, a simple approach was used (figure 4(c)). The empty space was approximated as a triangular prism, where the height is the radius (r) of the PS spheres, the width of the base line is $2r$, and the length of the Ag line is l. Thus, the volume can be approximated as r^2l. Based on this approximation, when r is reduced to $0.4r$ by heat pretreatment, the empty volume decreases to $0.16r^2l$. In other words, while the initial radius of the PS spheres decreases to 40% due to heat pretreatment, the empty volume decreases to 16% of the initial volume. Based on this calculation, we expect at least a 40% reduction in the total parasitic Ag island area. Thus, if the Ag ink concentration is 11.5 wt%, the Ag line thickness at the thinnest will be about one-ninth of the PS sphere radius, as shown in figure 4(a).

Three-micron PS sphere templates formed on PET substrate were annealed at 110 °C using a hot plate for various times. A temperature of 110 °C was selected considering the glass transition temperature of polystyrene (95 °C). As the PS spheres melted, and the triangular areas between three PS spheres decreased monotonically with heat pretreatment time (figure S4 available at stacks.iop.org/Nano/24/235205/mmedia). Based on multiple examinations of the 3 μm PS sphere template, we chose an optimum annealing time of 4 min, where the triangle area was about 0.07 μm^2.

The sheet resistance and transmittance as a function of heat pretreatment time for Ag honeycomb mesh fabricated using 3 μm PS spheres are given in figure 5(a). The transmittance increased linearly from 35% to 71% as the annealing time increased due to reduced Ag parasitic islands. Heat pretreatment improved the transmittance by about 7% in 2 min. The sheet resistance increased rapidly with annealing time. As a result, the annealing time should remain less than 4 min to obtain a sheet resistance below 50 Ω/sq. The rapid increase in sheet resistance is attributed to reduced Ag line thickness due to the reduced empty space. This problem can be solved by using larger PS spheres. FE-SEM images of the Ag honeycomb mesh fabricated using 3 μm PS spheres combined with heat pretreatment are given in figures 5(b)–(g) as a function of pretreatment time. As the heat pretreatment

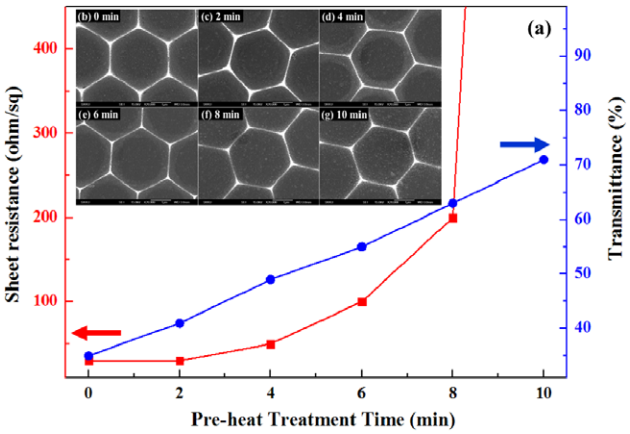

Figure 5. (a) Sheet resistance and transmittance of Ag honeycomb mesh fabricated using 3 μm PS spheres as a function of heat pretreatment time. FE-SEM images of Ag honeycomb mesh fabricated using 3 μm PS film after pretreatment at 110 °C for (b) 0 min, (c) 2 min, (d) 4 min, (e) 6 min, (f) 8 min, and (g) 10 min.

time increased from 0 to 10 min, the area occupied by parasitic Ag islands tended to decrease. The size of the Ag hexagon mesh equaled the PS sphere diameter, 3 μm. The Ag nanoparticle diameters ranged from 50 to 100 nm. As shown in figure 5(b), the line width in Ag honeycomb mesh fabricated without heat pretreatment was about 50 nm, and the line width including parasitic Ag islands was about 1000 nm. An FE-SEM image of Ag honeycomb mesh fabricated using a 4 min heat pretreatment is given in figure 5(d). A noticeable change in the line width of the Ag honeycomb mesh was not observed, but the line width including parasitic Ag islands decreased to 450 nm, less than half of that from mesh without heat pretreatment (1000 nm). An increase in the annealing time further reduced the Ag parasitic island areas, as shown in figures 5(e)–(g). However, the bright lines, which correspond to Ag lines of the mesh, remained the same width (about 50 nm). Consequently, the parasitic Ag island area decreased significantly with increasing heat pretreatment time up to 10 min.

Since the Ag mesh thickness is important in determining the sheet resistance, we analyzed the Ag honeycomb mesh using SPM (supporting information, figure S6 available at stacks.iop.org/Nano/24/235205/mmedia). The distance between two parallel Ag mesh lines was about 3 μm,

Table 1. Summary of the properties of Ag honeycomb mesh fabricated using 3 μm PS spheres.

Time (min)	Ag line thickness (nm)	Open ratio (%)	Transmittance (%)	Sheet resistance (Ω/sq)
0	197.0 ± 7.2	—	35	<30
2	175.7 ± 8.7	37.0	41	<30
4	161.0 ± 5.4	49.6	49	<50
6	113.1 ± 5.7	53.9	55	<100
8	101.3 ± 10.4	65.4	63	<200
10	69.8 ± 7.5	77.9	71	>2000

the diameter of a PS sphere. In addition, the Ag line thicknesses varied from 197.0 to 69.8 nm depending on the annealing time. The open ratio, which represents the proportionate Ag-free area in one hexagon, was measured from FE-SEM images (figure 5) using an image-processing program (TOMORO SCOPE-EYE). The Ag line thicknesses and open ratios are given in table 1 as a function of annealing time and are plotted in figure S7 (available at stacks.iop.org/Nano/24/235205/mmedia). As might be expected, the Ag line thickness decreased with annealing time, while the open ratio increased by up to 80% with annealing time. Although the open ratio does not exactly equal the transmittance, it was similar to the measured transmittance. As shown in table 1, when heat pretreatment was performed for more than 6 min, the sheet resistances were greater than 100 Ω/sq. The abrupt increase in sheet resistance can be explained by the rapid decrease in Ag line thickness. When the Ag line thickness was greater than 150 nm, the sheet resistance was typically less than 50 Ω/sq. In contrast, when the Ag line thickness was less than 150 nm, the sheet resistance was greater than 50 Ω/sq. Therefore, the minimum Ag line thickness to keep the sheet resistance below 50 Ω/sq is 150 nm.

Finally, Ag honeycomb mesh fabricated using 3 μm PS spheres pretreated for 4 min was used for a wet etching study to improve transmittance with good electrical conductivity. Figure 6(a) shows the variation in sheet resistance and transmittance as a function of the etching time. As shown in figure 6(a), in the early etching period (0–50 s) the transmittance increased rapidly due to eliminated oxide layers on Ag lines. This initial period (50 s), shown in figure 6(a), is shorter than the initial period (100 s) for the same sample without pretreatment (figure 3(d)) because many parasitic Ag islands were eliminated by heat pretreatment. The initial transmittance of Ag mesh fabricated using 3 μm PS spheres pretreated for 4 min was 49%, which is higher than the transmittance of Ag mesh fabricated using 3 μm PS spheres without pretreatment (35%, figure 3(d)). After 50 s, the transmittance increased with wet etching time because parasitic Ag islands near main Ag lines were eliminated relatively slowly. The sheet resistance decreased in the early etching period due to decreased Ag line thickness. This trend continued for etch times up to 700 s. After etching for 800 s, however, the sheet resistance increased rapidly to about 200 Ω/sq because some Ag lines started to break. FE-SEM images of Ag mesh obtained after wet etching for various times are given in figures 6(b)–(e). The figures clearly show that parasitic Ag islands were gradually eliminated by wet etching. The enlarged FE-SEM images indicate that wet

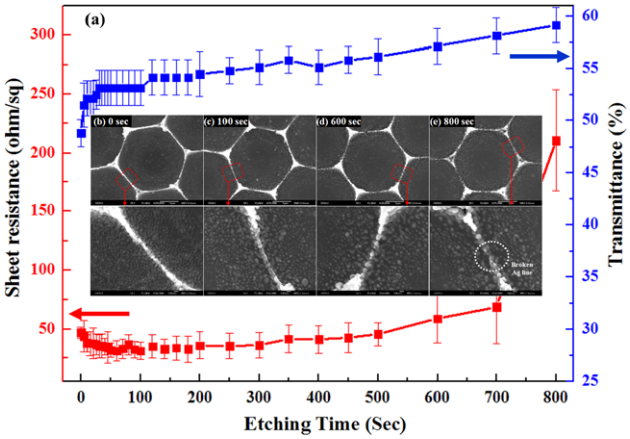

Figure 6. (a) Variations in sheet resistance and transmittance of Ag honeycomb mesh fabricated using 3 μm PS spheres and pretreated for 4 min as a function of wet etching time. FE-SEM images and enlarged images of Ag honeycomb mesh obtained after etching for (b) 0 s, (c) 100 s, (d) 600 s, and (e) 800 s. The enlarged FE-SEM image areas are indicated by dashed boxes.

etching reduced both the Ag parasitic area and the Ag line thickness. In addition, when the etching time was greater than 800 s, Ag lines broke, indicated by a dotted circle in figure 6(e). Therefore, the sheet resistance increased abruptly after Ag etching for 800 s.

The use of 3 μm PS spheres combined with both heat pretreatment and wet etching clearly improves transmittance with a low sheet resistance. To optimize sheet resistance, the Ag lines should be thicker than 150 nm, which is the minimum thickness for a resistance of 50 Ω/sq. To optimize transmittance, heat pretreatment is required to reduce the density of Ag parasitic islands. Heat pretreatment, however, involves a trade-off between optical transmittance and electrical conductivity. Shorter pretreatment gives thicker Ag lines, thereby lowering sheet resistance, but it comes at the expense of optical transmittance due to larger Ag parasitic islands. Therefore, 80% transmittance cannot be obtained with good electrical properties using 3 μm PS spheres because the Ag lines are too thin for good conductivity. Thus, larger PS spheres, e.g. 10 μm, are necessary for high transmittance with good electrical properties.

3.3. Heat pretreated, 10 μm PS spheres combined with wet etching

We first optimized the annealing time for heat pretreatment. As the annealing time increased, the triangle area decreased

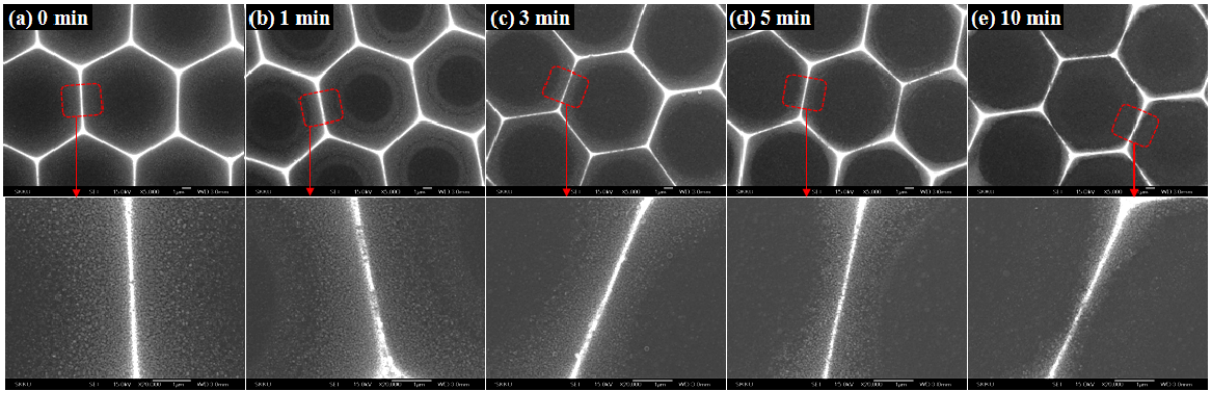

Figure 7. FE-SEM images of Ag honeycomb mesh obtained using 10 μm PS spheres with different annealing times: (a) 0 min, (b) 1 min, (c) 3 min, (d) 5 min, and (e) 10 min. The enlarged FE-SEM image areas are indicated by dashed boxes.

(supporting information, figure S8 available at stacks.iop.org/Nano/24/235205/mmedia). After 5 min, the PS spheres had melted, adhered, then formed a hexagonal pattern; therefore the triangle area was not detectable by FE-SEM. The measured areas were plotted as a function of annealing time; the plot of triangle area as a function of heat pretreatment time was similar to that in figure S4 (available at stacks.iop.org/Nano/24/235205/mmedia). The optimized annealing temperature was 150 °C, which is higher than that used for 3 μm PS spheres due to the larger size. Finally, Ag honeycomb meshes were fabricated with different heat pretreatment times, as shown in FE-SEM images (figure 7). The Ag hexagon size was equal to the diameter of the 10 μm PS spheres. As shown in figure 7(b), for 1 min pretreatment, the Ag mesh lines were about 100 nm wide, and parasitic Ag islands including Ag mesh lines were about 4400 nm wide. For 10 min pretreated samples, even though the Ag mesh line widths (100 nm) did not change, the parasitic Ag island widths, including the Ag mesh lines, decreased to 500 nm, as shown in figure 7(e). The area occupied by Ag parasitic islands decreased with pretreatment time. Based on FE-SEM image analysis, the optimum pretreatment time was 10 min. Compared to previous experiments using 3 μm PS spheres, the area of Ag parasitic islands decreased noticeably while the Ag hexagon line thickness increased. By SPM analysis (supporting information, figure S9 available at stacks.iop.org/Nano/24/235205/mmedia), the Ag line thickness before pretreatment was 576.3 nm, and the thickness after 10 min of annealing was 222.0 nm, which was thick enough to keep the sheet resistance below 50 Ω/sq, even after optimized wet etching. The measured Ag line thicknesses before and after wet etching were consistent with calculated values based on the height and Ag ink concentration. In other words, the Ag line thickness is about one-ninth of the PS sphere radius (5 μm) times the Ag ink concentration (11.5 wt%), or 570 nm. Similarly, the Ag line thickness after pretreatment for 10 min (222.0 nm) could be estimated by considering that the height of the highest empty space shrank from 5 to about 2 μm (2 μm × 11.5 wt% = 230 nm).

To determine the exact effect of pretreatment, SPM thickness profiles were obtained from SPM images plotted on a spreadsheet, as shown in figure 8. According to the

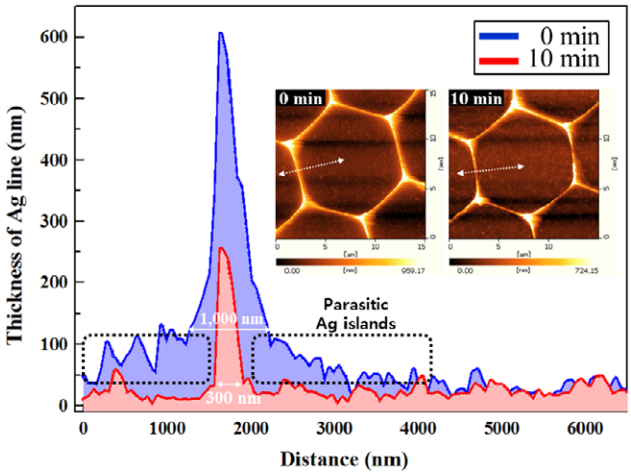

Figure 8. SPM images and line thickness profiles of Ag mesh fabricated using 10 μm PS spheres pretreated for (a) 0 min and (b) 10 min.

figure, pretreatment for 10 min decreased the Ag line width from about 1000 to 300 nm. Furthermore, it caused about a 100 nm decrease in the thickness; thereby the area of parasitic Ag islands, dotted boxes in the figure, decreased by 100 nm. Consequently, the sheet resistance and transmittance of Ag mesh samples pretreated for 10 min were 40 Ω/sq and 81%, respectively. Further improvement in the transmittance was possible using Ag wet etching.

Figure 9(a) shows the variation of the average sheet resistance and transmittance as a function of Ag etching time. As explained above, the sheet resistance decreased abruptly in the early etching period then increased as etching time increased. The transmittance increased slightly from 81% to 83% as wet etching proceeded due to fewer Ag parasitic islands. The effect of pretreatment is clear in figures 9(b) and (c). As shown in figure 9(b), parasitic Ag islands were mostly eliminated by a 10 min pretreatment. The remaining parasitic Ag islands near Ag lines were removed by wet etching for 200 s, as shown in figure 9(c). Wet etching for 200 s increased the sheet resistance from 20 to 35 Ω/sq by decreasing the Ag mesh thickness. The open ratios in figures 9(b) and (c) are 82.6% and 88.0%, respectively. The

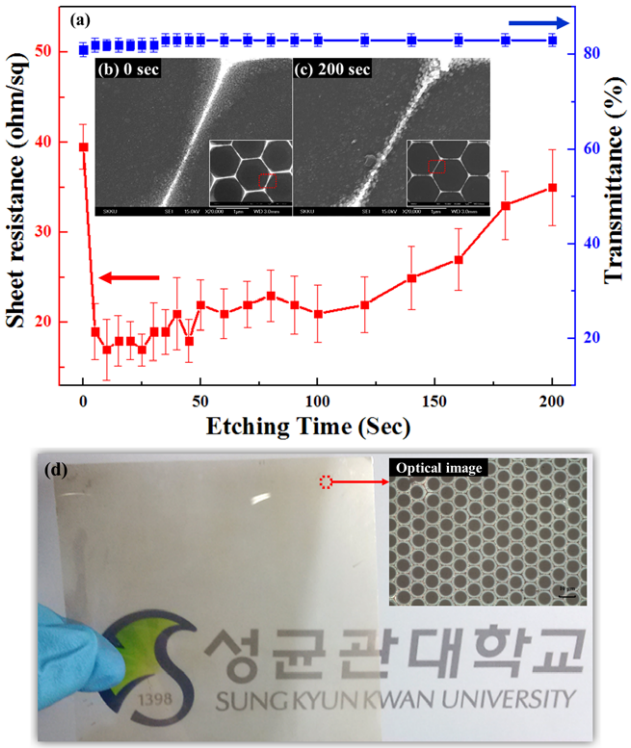

Figure 9. (a) Variation in the sheet resistance and transmittance of Ag honeycomb mesh fabricated using 10 μm PS spheres as a function of etching time. FE-SEM images and enlarged images of Ag honeycomb mesh after etching for (b) 0 s and (c) 200 s. The enlarged FE-SEM image areas are indicated by dashed boxes. (d) Optical images of Ag honeycomb mesh fabricated using 10 μm PS spheres.

open ratio was improved by only 5.4 percentage points by reducing parasitic Ag islands, while the transmittance was improved by 2 percentage points. The transmittance improved slightly after wet etching because most parasitic Ag islands were removed by the heat pretreatment. In addition, since the Ag triangle is more than twice as thick as the Ag lines, the Ag triangle areas occupy most of the hexagon structure and prevent further improvements in transmittance, thereby yielding a slight enhancement even after wet etching. Finally, figure 9(d) shows a photograph and optical image of Ag honeycomb mesh fabricated using 10 μm PS film on PET with dimensions, transmittance, and sheet resistance of 100 mm $\times$ 100 mm, 83%, and 20 Ω/sq, respectively.

4. Conclusions

We fabricated Ag honeycomb mesh transparent electrodes on a PET substrate using PS sphere templates and a lift-off process. The PS sphere diameters used in this study were 600 nm, 3 μm, and 10 μm. Since Ag parasitic islands reduced the transmittance, wet etching and heat pretreatment were used. Although heat pretreatment reduced parasitic Ag islands, it also increased the sheet resistance by reducing the Ag mesh thickness. To compensate for the trade-off between transmittance and sheet resistance, larger diameter PS spheres were required. Thus, 10 μm PS spheres were used as a template for Ag honeycomb mesh, and heat pretreatment and wet etching were combined to improve the transmittance and sheet resistance. The transmittance and sheet resistance were 83% and 20 Ω/sq, respectively. These properties could be further improved by optimization in future experiments. These transparent electrodes fabricated using a simple and low cost solution process seem to be an alternative for flexible electronics.

Acknowledgments

This research was supported by a grant from the Fundamental R&D Program for Technology of World Premier Materials funded by the Ministry of Knowledge Economy, Republic of Korea.

References

[1] Pang S, Hernandez Y, Feng X and Müllen K 2011 *Adv. Mater.* **23** 2779
[2] Hecht D S, Hu L and Irvin G 2011 *Adv. Mater.* **23** 1482
[3] Kumar A and Zhou C 2010 *ACS Nano* **4** 11
[4] Kim T, Kim Y W, Lee H S, Kim H, Yang W S and Suh K S 2012 *Adv. Funct. Mater.* **23** 1250
[5] Lee J, Connor S T, Cui Y and Peumans P 2008 *Nano Lett.* **8** 689
[6] MacDiarmid A G 2001 *Angew. Chem. Int. Edn* **40** 2581
[7] Vosgueritchian M, Lipomi D J and Bao Z 2012 *Adv. Funct. Mater.* **22** 421
[8] Zhu Y and Xu F 2012 *Adv. Mater.* **24** 1073
[9] Salvatierra R V, Cava C E, Roman L S and Zarbin A J G 2012 *Adv. Funct. Mater.* **23** 1490
[10] Bae S *et al* 2010 *Nature Nanotechnol.* **5** 574
[11] Indluru A and Alford T L 2009 *J. Appl. Phys.* **105** 123528
[12] Chiba K and Futagami A 2008 *Appl. Phys. Lett.* **93** 013114
[13] De S *et al* 2009 *ACS Nano* **3** 714
[14] Zhu R *et al* 2011 *ACS Nano* **5** 9877
[15] Chang H, Wang G, Yang A, Tao X, Liu X, Shen Y and Zheng Z 2012 *Adv. Funct. Mater.* **20** 2893
[16] Woerle J and Rost H 2011 *MRS Bull.* **36** 789
[17] Kang M and Guo L J 2007 *Adv. Mater.* **19** 1391
[18] Kuang P, Park J, Leung W, Mahadevapuram R C, Nalwa K S, Kim T, Chaudhary S, Ho K and Constant K 2011 *Adv. Mater.* **23** 2469
[19] Ho Y, Chen K, Liu S, Chang Y, Huang D and Wei P 2011 *Org. Electron.* **12** 961
[20] Cheng K, Cui Z, Li Q, Wang S and Du Z 2012 *Nanotechnology* **23** 425303
[21] Kei C, Kuo K, Su C, Lee C, Hsiao C and Perng T 2006 *Chem. Mater.* **18** 4544
[22] Li H, Low J, Brown K S and Wu N 2008 *IEEE Sensors J.* **8** 880
[23] Jeong G H, Park J K, Lee K K, Jang J H, Lee C H, Kang H B, Yang C W and Suh S J 2010 *Microelectron. Eng.* **87** 51
[24] Johnson L and Walsh D A 2011 *J. Mater. Chem.* **21** 7555
[25] Madaria A R, Yao M, Chi C, Huang N, Lin C, Li R, Povinelli M L, Dapkus P D and Zhou C 2012 *Nano Lett.* **12** 2839
[26] Hulteen J C and Van Duyne R P 1995 *J. Vac. Sci. Technol.* **13** 1553
[27] Frey W, Woods C K and Chilkoti A 2000 *Adv. Mater.* **12** 1515
[28] Ye J Y, Li Y Q, Gao J, Peng H Y, Wu S X and Wu T 2010 *Appl. Phys. Lett.* **97** 132108
[29] Zhu J, Zhu X, Hoekstra R, Li L, Xiu F, Xue M, Zeng B and Wang K L 2012 *Appl. Phys. Lett.* **100** 143109